CANDIDATE RECEIVERS FOR UNBALANCED QPSK

CHARLES L. WEBER
University of Southern California
Los Angeles, California

Summary. Candidate receivers for unbalanced QPSK signal foremats have been studied. The fourth power receiver is shown to be an unsatisfactory choice unless the power division is close to 50-50 or 100-0. The Costas loop receiver which tracks on the high data rate signal of the unbalanced QPSK waveform is shown to perform satisfactorily. Approximate error rate computations, show that the Costas loop considered performs within a few tenths of a dB of the ideal receiver.

Introduction. We consider various candidate receivers for the unbalanced QPSK signal format. The basic modulator configuration is shown in Figure 1. The transmitted signal is

$$s(t) = Aa(t) \cos \omega_0 t + Bb(t) \sin \omega_0 t \tag{1}$$

where a(t) = ±1 represents the encoded data of the high rate, or I, channel and b(t) = ±1, asynchronous to a(t), represents the encoded data in low rate, or Q, channel. We shall consider the effects of both NRZ and Bi-φ-L waveforms.

The purpose of an unequal power ratio is to cause the symbol energy, and therefore the error rates, in the two channels to be closer to the same value. When the data rates differ significantly, e.g. 10:1, little is gained by unbalancing the power by more than 4:1. From an error rate point of view, this overpowers the low rate data channel. The maximum to be gained however, by placing all the power in the high rate channel with respect to a 4:1 power division is less than 0.1 dB.

Fourth-Power Receiver Tracking Loop. A block diagram of the fourth-power tracking loop is shown in Figure 2. The signal at the input to the fourth-power device is y(t) = s(t) + n(t), where s(t) is given by (1) and the narrowband noise is

$$n(t) = \sqrt{2}[n_c(t) \cos \omega_0 t + n_s(t) \sin \omega_0 t] \tag{2}$$

The independent baseband noises, $n_c(t)$ and $n_s(t)$ are the projections of n(t) in the cosine and sine directions respectively. Each has one-sided spectral density N_0 watts/hertz and bandwidth $B_{IF}/2$.

The difficulties associated with the fourth-power tracking loop can be demonstrated without considering the additive noise when the power division is near 4:1. With signal only, the output of the fourth-power device in Figure 2 is

$$y^4(t) = s^4(t)$$

$$= \left(\frac{A^4+B^4}{8}\right) \cos(4\omega_0 t) + \left(\frac{A^4-B^4}{8}\right)\cos(2\omega_0 t) + 3\left(\frac{A^4+B^4}{8}\right) +$$

$$+ \tfrac{1}{2}a(t)b(t)\{A^3B[\sin(4\omega_0 t)-\sin(2\omega_0 t)] - AB^3[\sin(4\omega_0 t)+\sin(2\omega_0 t)]\}$$

$$+ \frac{3}{2}(A^3B+AB^3)\sin(2\omega_0 t) + \frac{3}{4}A^2B^2[1 - \cos(4\omega_0 t)] \qquad (3)$$

After passing the BPF centered at $4f_0$ in Figure 2, the result is

$$z(t) = \frac{A^4+B^4-6A^2B^2}{8}\cos(4\omega_0 t) + \frac{a(t)b(t)}{2}(A^3B-AB^3)\sin(4\omega_0 t) \qquad (4)$$

The first term in (4) is the tracking term, and the second term represents self-generated noise. In terms of the average power in each link, namely $P_A = A^2/2$ and $P_B = B^2/2$, z(t) is

$$z(t) = \tfrac{1}{2}[P_A^2 + P_B^2 - 6P_AP_B]\cos(4\omega_0 t) + 2a(t)b(t)\sqrt{P_AP_B}(P_A-P_B) \cdot \sin(4\omega_0 t) \qquad (5)$$

The tracking term is $\cos(4\omega_0 t)$ and contributes a spectral component at 4wot. The other term is self-noise, which contributes a spectral density at $4\omega_0 t$. The level of the spectral density within the tracking loop receiver is dependent on the signal waveforms chosen for a(t) and b(t).

The tracking power is

$$P_{track} = \frac{1}{8}[P_A^2 + P_B^2 - 6P_AP_B] \qquad (6)$$

The self -noise power in the tracking loop is equal to the spectral density of the second term in (5) at $4f_0$ times the tracking loop bandwidth, which is expressed by

$$P_{SN} = 4P_AP_B(P_A-P_B)^2S(0)B_L \qquad (7)$$

where B_L is the tracking loop noise bandwidth and S(0) is the two-sided spectral density of the signal a(t)b(t) at f=0. When a(t) is NRZ with symbol time T_A and b(t) is Bi-φ-L with symbol time T_B , then

$$S(0) = T_A(1 - T_A/T_B) \tag{8}$$

When a(t) and b(t) are both Bi-φ-L then

$$S(0) = T_A^2/(2T_B) \tag{9}$$

In order to obtain a preliminary evaluation of the performance of the fourth-power tracking loop, let the total power be P_T, and

$$P_A = \alpha P_T \qquad P_B = (1-\alpha)P_T \tag{10}$$

The ratio of tracking power to self-noise power within the tracking loop is then given by

$$\frac{P_{track}}{P_{SN}} = \frac{1}{32} \frac{[P_A^2 + P_B^2 - 6P_AP_B]^2}{P_AP_B[P_A-P_B]^2 2S(0)B_L}$$

$$= \frac{1}{32} \frac{N}{D[2S(0)]B_L} \tag{11}$$

where

$$N = [\alpha^2 + (1-\alpha)^2 - 6\alpha(1-\alpha)]^2 \tag{12}$$

$$D = \alpha(1-\alpha)[\alpha - (1-\alpha)]^2 \tag{13}$$

The parameter α represents the fraction of total power in the high data rate link, which assumes values over $0.5 \le \alpha \le 1$. The numerator N in (11) and (12) represents the variation in tracking power as a function of the power division and is shown in Figure 3 as the dashed line. The denominator D represents the variation in self-noise spectral density as a function of the power division. The denominator is also shown in Figure 3, where it can be seen that D reaches a maximum and N a minimum of 0 near $\alpha = 0.85$. The variation of the ratio of signal power to self-noise spectral density

$$\frac{N}{32D} = 2B_L S(0) \frac{P_{track}}{P_{SN}} \tag{14}$$

is also shown in Figure 3, where it is noted that the worst power divisions are within [0.8,0.9]. It is seen that the fourth power tracking loop makes very ineffective use of the total available tracking power when the power division is in the interval [0.65,0.95], which includes most values of α. An additional disadvantage of the fourth-power tracking loop is that the stable lock points occur at multiples of π/4, thereby allowing the possibility that the two data channels become interchanged. This could be detected and alleviated in a system design, but only at the expense of additional complexity.

With these results, we conclude that the fourth-power tracking loop should not be recommended for the generation of a coherent reference of an unbalanced QPSK signal when $\alpha > 0.6$.

Costas Receiver. A block diagram of the Costas Loop receiver for unbalanced QPSK is shown in Figure 4. The reference signals are given by

$$r(t) = \sqrt{2}\cos(\omega_0 t+\varphi) \qquad r'(t) = \sqrt{2}\sin(\omega_0 t+\varphi) \tag{15}$$

Under the assumption that the IF filter preceding the Costas loop receiver is sufficiently wide to pass both channels of the received signal without distortion, then the baseband outputs $e_c(t)$ and $e_s(t)$ of the mixers, neglecting $2f_0$ terms are

$$\begin{aligned} e_c(t) &= (1/\sqrt{2})[Aa(t)\cos\varphi - Bb(t)\sin\varphi] + n_c(t) \\ e_s(t) &= (1/\sqrt{2})[Aa(t)\sin\varphi + Bb(t)\cos\varphi] + n_s(t) \end{aligned} \tag{16}$$

In specifying the bandwidth B_1 of the LPF's in each arm of the Costas loop, we assume B_1 is at least as large as the bandwidth of a(t) and b(t). This is equivalent to saying the tracking loop is going to function primarily on the high-rate, high-powered channel. The dynamic error signal e(t) is then given by

$$\begin{aligned} e(t) &= e_c(t)e_s(t) \\ &= \left(\frac{P_A - P_B}{2}\right)\sin(2\varphi) && \left.\begin{matrix}\\ \end{matrix}\right\} \text{Tracking Signal} \\ &\quad + \sqrt{P_A P_B}\, a(t)b(t)\cos 2\varphi && \left.\begin{matrix}\\ \end{matrix}\right\} \text{Self-Noise} \\ &\quad + n_c(t)\, n_s(t) && \left.\begin{matrix}\\ \end{matrix}\right\} \text{Noise} \\ &\quad + n_c(t)[\sqrt{P_A}\, a(t)\sin\varphi + \sqrt{P_B}\, b(t)\cos\varphi] && \left.\begin{matrix}\\ \\ \end{matrix}\right\} \text{S}\times\text{N} \\ &\quad + n_s(t)[\sqrt{P_A}\, a(t)\cos\varphi - \sqrt{P_B}\, b(t)\sin\varphi] && \end{aligned} \quad \left.\begin{matrix}\\ \\ \\ \\ \end{matrix}\right\} n_{eq}(t) \tag{17}$$

where, in addition to the desired tracking signal, self -noise, noise and signal χ noise terms are generated, which we designate as the equivalent loop noise, $n_{eq}(t)$.

Observation of the tracking signal in (17) provides the following:

i) The stable lock points are at $\varphi = \pm k\pi$, with the result that the two data sequences cannot be sent to the incorrect data demodulator.

ii) Although it is usually expected that the power in both channels will always be present even if the data rates are reduced to zero, should the power in the high data rate channel fail, i. e. $P_A \rightarrow 0$, then the sign of the tracking signal is reversed and the stable lock angles are at $\pi/2 \pm k\pi$. If this occurs, then the low data rate link win be processed into the high data rate demodulator.

iii) If the power in the low data rate link goes to zero, i. e. , $P_B \rightarrow 0$, the stable lock angles remain unchanged, so that the high data rate link continues to be processed into the high data rate demodulator.

The statistics of the equivalent noise, $n_{eq}(t)$, are obtained by assuming that the tracking loop bandwidth is much smaller than B_1. The phase error $\varphi(t)$ will then be slowly varying with respect to the other random processes present in e(t). The first and second conditional moments are given by

$$E[n_{eq}(t)|\varphi] = 0 \tag{18}$$

and

$$\begin{aligned} R_{n_{eq}}(\tau) &= E[n_{eq}(t)n_{eq}(t+\tau)|\phi] \\ &= P_A P_B R_a(\tau)R_b(\tau)\cos^2(2\varphi) \\ &\quad + R^2(\tau) + R_N(\tau)[P_A R_a(\tau) + P_B R_b(\tau)], \end{aligned} \tag{19}$$

where $R_a(\tau)$ and $R_b(\tau)$ are the autocorrelation functions of a(t) and b(t), respectively.

The spectral density of $n_{eq}(t)$ is essentially flat over the bandwidth of the tracking loop, so that the significant statistic when considering tracking loop performance is the spectral density at f = 0. The spectral density of the terms in (19) are

$$R_N^2(\tau) \rightarrow S(0) = \int_{-B_1}^{B_1} (N_0/2)^2 df = \frac{N_0^2 B_1}{2} \tag{20}$$

$$R_N(\tau)[P_A R_a(\tau) + P_B R_b(\tau)] \rightarrow S(0) \approx \frac{N_0}{2}(P_A + P_B) \tag{21}$$

$$P_A P_B R_a(\tau)R_b(\tau)\cos^2(2\varphi) \rightarrow S(0) \approx P_A P_B T_A \left(1 - \frac{T_A}{T_B}\right) \tag{22}$$

where in (22), we have imposed the upper bound, $\cos^2(2\varphi) \leq 1$. When a(t) is NRZ and b(t) is Bi-φ-L, the two-sided spectral density of $n_{eq}(t)$ is

$$S_{n_{eq}}(0) \triangleq \frac{N_{0_{eq}}}{2} = \frac{N_0^2 B_1}{2} + \frac{N_0}{2}(P_A + P_B) + P_A P_B T_A \left(1 - \frac{T_A}{T_B}\right) \tag{23}$$

We shall base our performance analyses on a linearized assumption. At the high IF signal-to-noise ratios which are assumed, the Costas loop is well within its linearized region. When such is the case, the variance of the phase error can be approximated by

$$\sigma_\varphi^2 = \tfrac{1}{4}\sigma_{2\varphi}^2 = \frac{1}{4\rho} \ (\text{rad})^2 \tag{24}$$

where ρ is the signal-to-noise ratio in the Costas loop, which is given by

$$\rho = \frac{P_c}{N_{0_{eq}} B_L} \tag{25}$$

where P_c is the available power in watts for tracking, B_L is the one-sided equivalent noise bandwidth of the tracking loop in Hz, and $N_{0_{eq}}$ is the one-sided spectral density of the equivalent additive noise in the loop in watts/Hz.

In our receiver, $N_{0_{eq}}$ is given by (23) and from (17)

$$P_c = (P_A - P_B)^2/4 \ . \tag{26}$$

Upon substitution og (23) and (26) into (25), the Costas loop signal-to-noise ratio is given by

$$\rho = \frac{(P_A - P_B)^2/4}{N_0 B_L \left[N_0 B_1 + P_A + P_B + \frac{2P_A P_B}{N_0} T_A \left(1 - \frac{T_A}{T_B}\right)\right]} \ . \tag{27}$$

Using the power division parameter α, as given by (10),

$$\rho = \frac{P_T}{4N_0 B_L} \left[\frac{(2\alpha - 1)^2}{1 + \frac{N_0 B_1}{P_T} + \frac{2P_T \alpha(1-\alpha)}{N_0} T_A \left(1 - \frac{T_A}{T_B}\right)}\right] \tag{28}$$

The performance of the Costas tracking loop when tracking on the high-powered channel is then given by (24) and (28), and is shown in Figure 5. The standard deviation of the phase error is shown versus the power division parameter α. Two sets of curves are

shown. Set (1) shows performance for the symbol rates R_A = 384 ksps and R_B = 192wps. This is a poor set of rates from the point of view of maximizing the standard deviation of the phase error. As shown, the two curves are for loop bandwidths of 5 kHz and 10 kHz. As $\alpha \rightarrow 0.5$, the Costas loop is unable to track and $\sigma \rightarrow \infty$. As $\alpha \rightarrow 1$, the signal becomes single channel, the high data rate channel, and the self-noise goes to zero. The effect of the self-noise can be determined by comparing the standard deviation at some α to that at $\alpha = 1$. The increase is due to the effects of the self-noise, and the fact that the available tracking power is also decreasing.

The second set of curves in Figure 5 is for a good set of rates. The improvement due to the resulting reduction in self-noise at the higher symbol rates is seen to be approximately an order of magnitude in σ. The points on the curves corresponding to $\alpha = 0.8$, a 4to-1 power division, have been emphasized by dots.

When both a(t) and b(t) are Bi-φ-L, the equivalent spectral density is given by

$$S_{n_{eq}}(0) = \frac{N_{0_{eq}}}{2} = \frac{N_0^2 B_1}{2} + \frac{N_0}{2}(P_A + P_B) + \frac{P_A P_B T_A^2}{2T_B} . \tag{29}$$

The resulting signal-to-noise ratio in the tracking loop bandwidth is then given by

$$\rho = \frac{P_T}{4N_0 B_L} \left[\frac{(2\alpha - 1)^2}{1 + \frac{N_0 B_1}{P_T} + \frac{P_T T_A^2}{N_0 T_B} \alpha(1-\alpha)} \right] . \tag{30}$$

The performance of the Costas loop for the forward link employing the high data rate link is then given by (30) and (24).

The performance when both a(t) and b(t) are Bi-φ-L is shown in Figure 6. The RMS phase error in degrees is again shown versus the power division for the unbalanced QPSK signal.

The set of curves designated (3) gives performance for a good set of rates from the RMS phase error point of view. The set of curves (4) gives tracking performance for a poor set of rates.

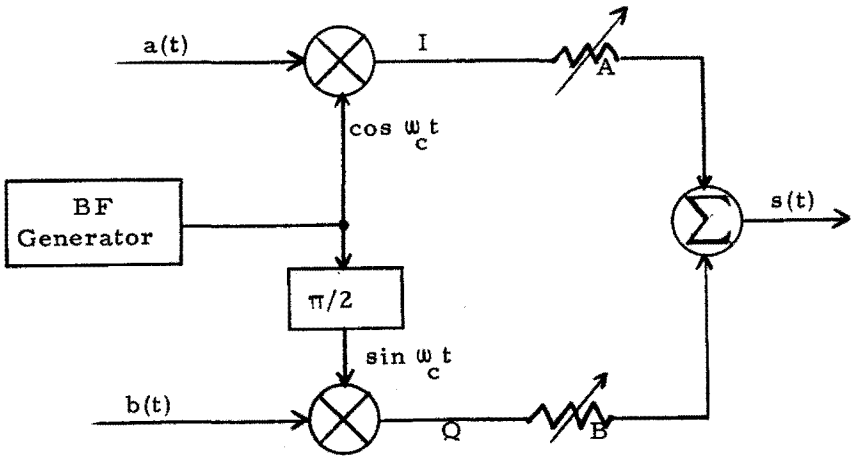

Figure 1. Unbalanced Quadriphase Modulator.

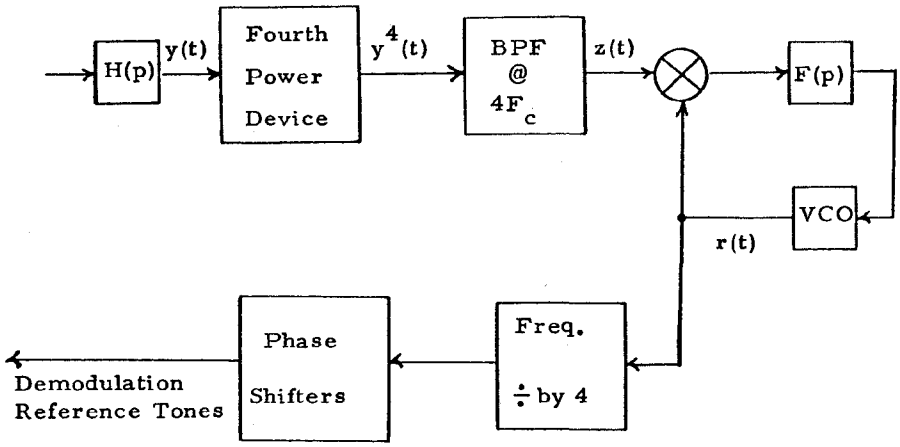

Figure 2. Fourth-Power Receiver Tracking Loop

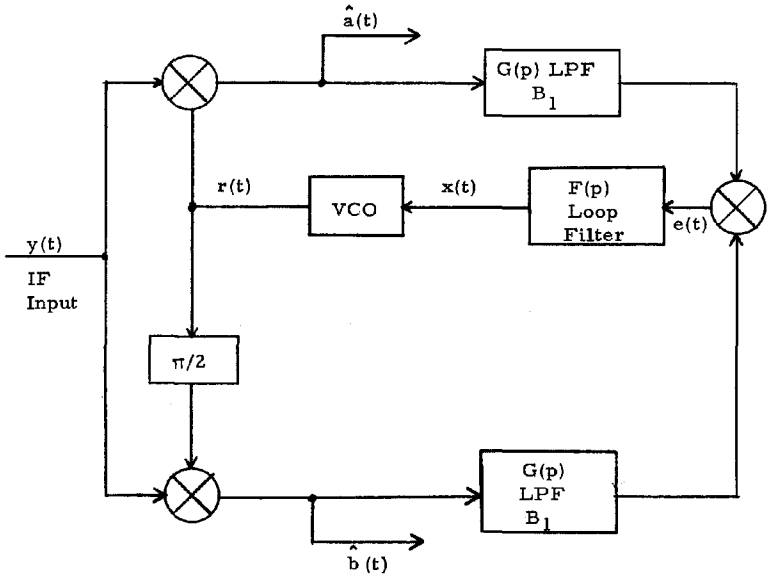

Figure 4. Costas Loop Quadriphase Receiver.

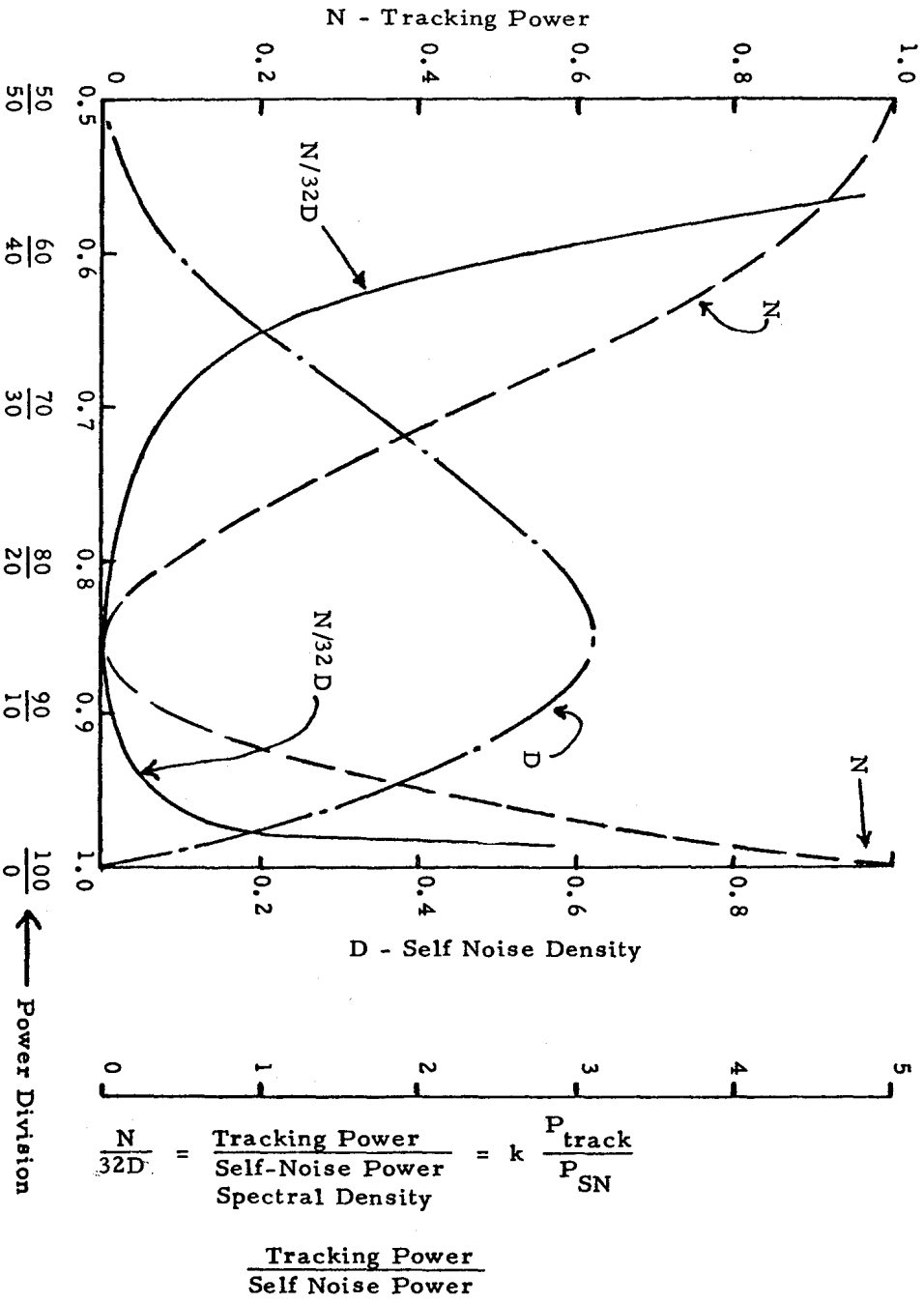

Figure 3. Tracking Power, Self Noise Density and Ratio of Tracking Power to Self Noise Density for the Fourth Power Tracking Loop.

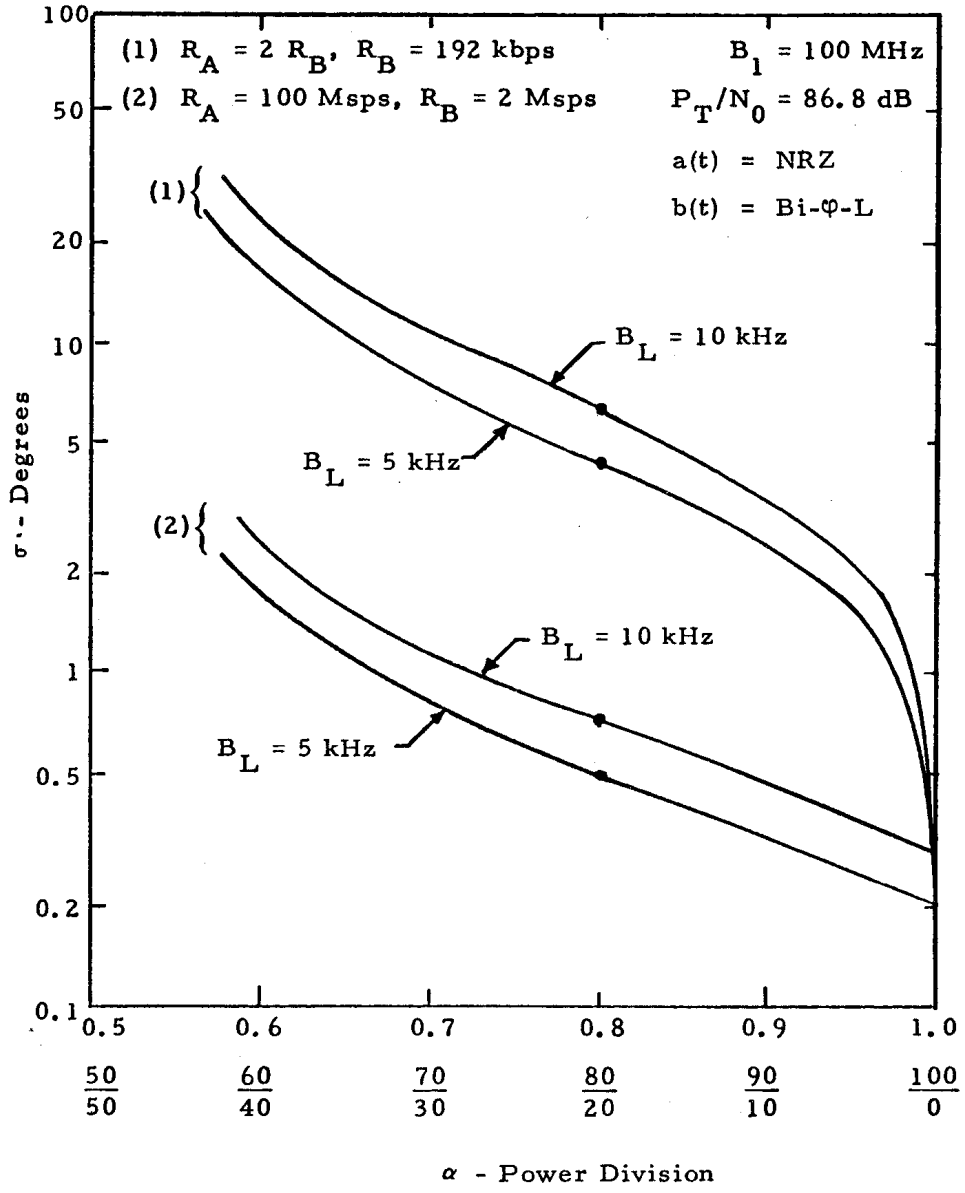

Figure 5. RMS Phase Error Versus Power Division for Unbalanced QPSK for the Return Link

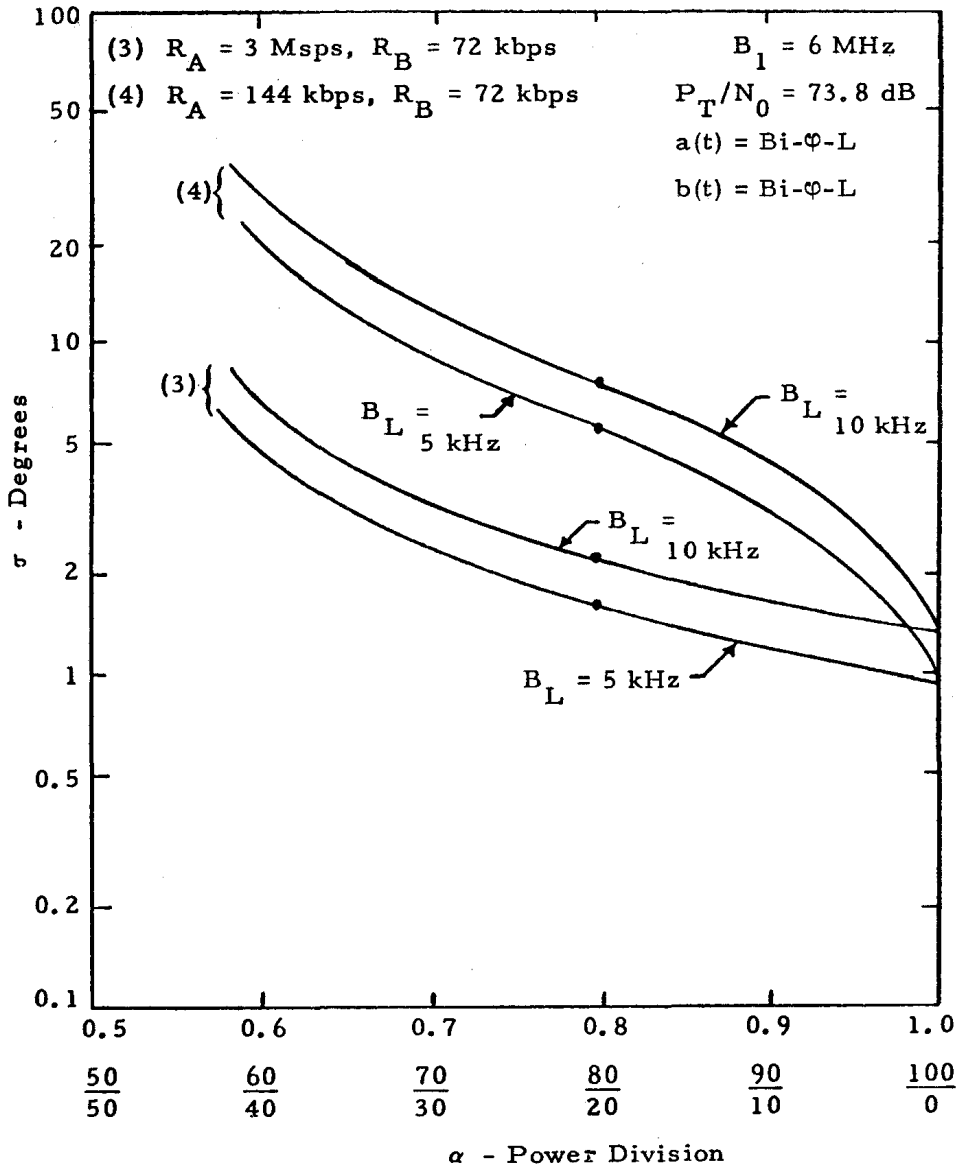

Figure 6. RMS Phase Error Versus Power Division for Unbalanced QPSK for the Forward Link